

Model for nanopillar growth by focused helium ion-beam-induced deposition

Paul F. A. Alkemade^{a)} and Ping Chen

Kavli Institute of Nanoscience, Delft University of Technology, Lorentzweg 1, 2628 CJ Delft, The Netherlands

Emile van Veldhoven and Diederik Maas

TNO Science and Industry, Stieltjesweg 1, 2628 CK Delft, The Netherlands

(Received 27 July 2010; accepted 11 October 2010; published 1 December 2010)

An analytical model for the growth of nanopillars by helium ion-beam-induced deposition is presented and compared to experimental data. This model describes the competition between pillar growth in vertical and lateral directions. It assumes that vertical growth is induced by incident primary ions and type-1 secondary electrons, whereas lateral growth is induced by scattered ions and type-2 secondary ions. An essential element of the model is the notion that depletion of adsorbed precursor molecules occurs only at the pillars' apex. Depletion impedes vertical growth at the apex, allowing more time for lateral outgrowth of the pillar's sidewalls. The model describes qualitatively the trends in measured vertical, lateral, and volumetric growth rates of PtC pillars as functions of the ion-beam current. It can be used to design growth experiments and Monte Carlo simulations. © 2010 American Vacuum Society. [DOI: 10.1116/1.3517536]

I. INTRODUCTION

Electron-beam-induced deposition (EBID) and ion-beam-induced deposition (IBID) are direct writing technologies in which precursor molecules adsorbed on a surface are decomposed by a beam-induced reaction, resulting in localized material deposition.¹ Pillars grow when a stationary beam is used. In general, EBID pillars are narrow, but their growth rate and purities are low. So far, most IBID pillars have been grown with Ga⁺ ion beams. The efficiency of Ga-IBID is relatively high in terms of number of atoms deposited per ion. Moreover, the materials are purer, though often contaminated with Ga. However, Ga-IBID pillars are often rough and much broader and blunter than EBID pillars.² Until recently, ion beams other than Ga had not been explored for pillar growth.

Helium ion microscopy (HIM) with a subnanometer probe size recently became available commercially.³ Apart from small probe sizes, the advantages of HIM include the narrow interaction volume in the substrate and the predominance of type-1 secondary electron emission.^{3,4} A helium ion microscope can also be used for nanofabrication.^{5,6} Sanford *et al.* showed that introducing a Pt-containing precursor gas into a helium ion microscope causes a deposit to form at the area exposed to the He⁺ beam.⁶ The deposition yield, i.e., the volume deposited per incident ion, of He-IBID is similar to that of Ga-IBID, although the Pt content is lower—at most 20 at. %, i.e., comparable to that of EBID.

Material growth by IBID is intimately linked to the trajectories and the energy losses of the particles in the growing material. If heavy ion beams are used, the nuclear energy losses cause atom removal from the bombarded areas, a process known as sputtering. This concomitant sputtering during

deposition makes it difficult to study Ga-IBID pillar growth. In contrast, sputtering rates for He⁺ beams are about two orders of magnitude lower and can, in a first approximation, be neglected in He-IBID.

Simulation work for EBID has resulted in a good qualitative understanding of the relevant processes.⁷ However, the lack of fundamental data on the precursor molecule decomposition and the fact that numerous types of possibly active particles may be present (incident and scattered electrons, and low-energy secondary electrons excited by the incident electrons—type 1—or by the scattered electrons—type 2) obstructed the quantitative and detailed understanding of EBID. Monte Carlo simulations offer, in principle, the best approach to model growth. Although they provide details of the processes, the outcome of simulations might be as complex as actual experiments. Therefore, simplified analytical models and dedicated experiments are helpful to study the most important quantities and basic processes.

In this article, we present a simple analytical model for the growth of narrow pillars with a stationary, nanometer-sized He⁺ beam. Our model is based on the idea that precursor depletion at the pillars' apex impedes vertical growth, allowing more time for lateral growth.⁷ The processes described in this work are related to EBID, but the primary particles are different and the yields of low-energy secondary electrons are higher. The processes are also related to IBID, but there is no sputtering.

II. EXPERIMENT

These experiments were performed in a Carl Zeiss OrionTM Plus scanning helium ion microscope equipped with an OmniGIS unit from Omniprobe. This gas-injection unit provides a continuous flow of (CH₃)₃Pt(C_pCH₃) and a N₂ carrier gas via a nozzle positioned 500 μm above the sample

^{a)}Electronic addresses: p.f.a.alkemade@tudelft.nl

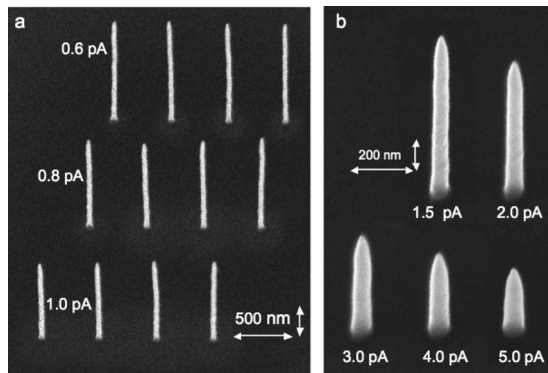


FIG. 1. Pillars grown with 25 keV He⁺ beams at various currents. The dose is 6.0 pC. Pillars grown at the lowest current are highest and thinnest.

surface. The temperature of the gas reservoir was 30 °C during deposition. The estimated precursor flux at the beam impact site was 3 molecules nm⁻² s⁻¹.⁸ The background pressure in the chamber was 6.3×10^{-7} mbar and the pressure during deposition was 4.5×10^{-6} mbar. Deposition was achieved with a stationary 25 keV He⁺ beam at normal incidence. Imaging with this beam showed that the beam width was less than 1 nm. The substrate material was Si with a native oxide. The current dependence of the pillar growth was studied between 0.6 and 5.0 pA for a total dose Q of 6.0 pC per deposit. The current was varied by regulating the helium pressure in the source. In each run, four deposits were made sequentially under the same conditions and were subsequently imaged at 0° and 30° sample tilt.

III. RESULTS

HIM images of nanopillars grown at different currents but with the same ion dose are shown in Fig. 1; more results are shown in Ref. 9. All deposits made at high currents are shaped like cones, whereas those made at low and intermediate currents are shaped like pillars, i.e., cylinders with conical tops. The thinnest pillars have a full width at half maximum (FWHM) of 36 ± 2 nm. Note that the conical top of the pillars is 100–150 nm long. The pillar height increases proportionally with time, whereas, apart from the initial

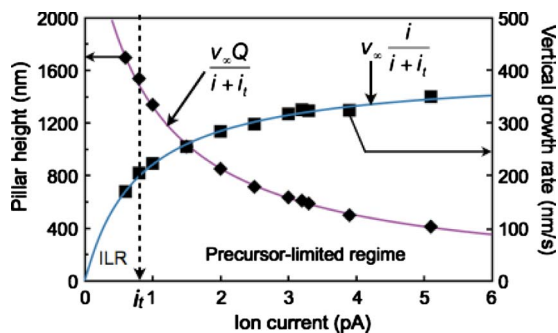


FIG. 2. (Color online) Pillar height H and vertical growth rate v_v vs ion-beam current i . ILR=ion-limited regime; i_t is the current that separates the ion-limited and the precursor-limited regimes. The solid curves are model fits (see text).

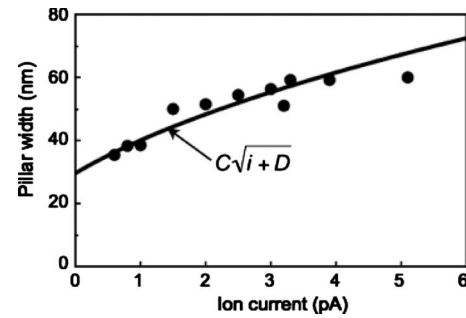


FIG. 3. Pillar width at half maximum vs ion current i . The curve is a model fit (see text).

phase, the pillar width remains constant.⁹ Figure 2 shows the height H and the vertical growth rate $v_v(=H \cdot i/Q)$ of the deposits as functions of the primary beam current i . Figure 3 shows the FWHM and Fig. 4 shows the deposited volume V^* per incident ion. The volume was calculated by integrating the area in the pillar images. Owing to the unfavorable viewing direction, the estimated error in the pillar volume ranges from 5% for the high, narrow pillars to 15% for the short, conical ones. The general result shown in Figs. 2–4 is that with increasing beam current, the deposits become shorter and broader, whereas their volume decreases only slightly.

IV. DISCUSSION

Pillars grow in two stages: first, as a cone and, subsequently, as a cone with a cylindrical base.⁹ For the conditions investigated here, the pillars' vertical growth rate is constant in time.⁹ The rate $v_v(i)$ increases with increasing beam current i , but it levels off at higher currents (Fig. 2). This behavior is characteristic of the transition from an ion-limited growth regime (ILR) to a precursor-limited regime.¹ The transient growth rate^{1,10} is

$$v_v(i) = \frac{v_\infty i}{i + i_t}, \quad (1)$$

where the parameter i_t can be regarded as the transition current between the two regimes and v_∞ is the growth rate in the extreme precursor-limited regime.

Furthermore,

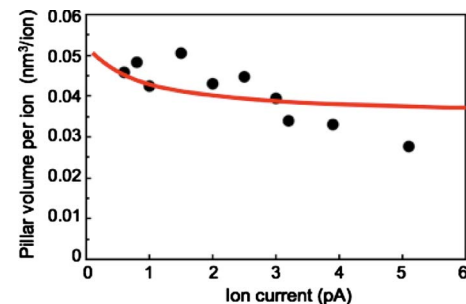


FIG. 4. (Color Online) Deposition efficiency or pillar volume V^* per incident ion vs ion current i . The solid curve is a model fit (see text).

$$H(i) = v_v(i)t_d = v_v(i)\frac{Q}{i} = \frac{v_\infty Q}{i + i_t}, \quad (2)$$

where t_d is the total deposition time. The solid curves in Fig. 2 are fits to the data with $v_\infty = 400 \pm 15$ nm/s and $i_t = 0.80 \pm 0.07$ pA. Clearly, the supply of precursor molecules to the growing pillar top falls short at almost all beam currents used. However, this slowing down does not apply to the volumetric growth rate shown in Fig. 4. Apparently, the supply of precursor molecules to the *entire* pillar is sufficient at almost all currents. The apex of the pillar is supplied with precursor molecules via direct adsorption from the gas phase and via surface diffusion across the pillar sidewall. The sidewall in turn is supplied via direct adsorption and diffusion from the substrate. The drop in the vertical growth rate and the constancy of the volumetric growth rate reveal details of the growth mechanism, which we will discuss in more detail below.

Simulation studies by Smith *et al.* found that in EBID and in He-IBID, the primary projectiles and the secondary electrons of type 1 (SE-1) dominate vertical pillar growth, whereas forward-scattered projectiles and secondary electrons of type 2 (SE-2) dominate lateral growth.^{7,10} Note that we define SE-1 here as the electrons emitted by the ions that enter the solid, whereas SE-2 by those that leave the solid. The escape depth of excited electrons is only a few nanometers.⁷ Hence, electrons that are excited in the interior of the pillar will not reach the surface and do not contribute to precursor decomposition. We use these concepts to explain the trends in Figs. 2–4. The lateral spread, or straggling, of 25 keV He ions in *flat* Pt₂₀C₈₀ [~ 100 nm (Ref. 9)] is much larger than the pillar radius (< 40 nm). Therefore, we assume that most ions penetrating the growing pillar also escape from it. Deposition will only take place in the region where ions enter or leave the pillar, thus not farther than the ion range R below the beam impact site, viz., the pillar's apex. Indeed, the range of ~ 200 nm (Ref. 9) agrees well with the observed height of 100–150 nm of the conical tops. The time t_L available for lateral growth is thus

$$t_L(i) = \frac{R}{v_v(i)} = \frac{R}{v_\infty} \left(1 + \frac{i_t}{i}\right). \quad (3)$$

Note that Eq. (3) is only valid if $t_L < t_d$. Of course, more SE-2s are produced per second at higher currents. Therefore, higher currents imply more lateral growth unless the growth time t_L is proportionally shorter. However, for the saturated growth at $i \gg i_t$, the growth time is fixed at R/v_∞ .

Figure 5 illustrates the two types of basic pillar growth processes. For simplicity, we will consider henceforth only decompositions induced by SE-1 and SE-2. The contributions of the primary and the scattered ions are qualitatively equivalent to those of SE-1 and SE-2, respectively, and do not influence the qualitative behavior of vertical and lateral growth. The local rate of growth in the direction perpendicular to the local surface is equal to the product of the volume increase ΔV per decomposition event, the local flux Φ_i of particles of type i , the local precursor surface density n , and

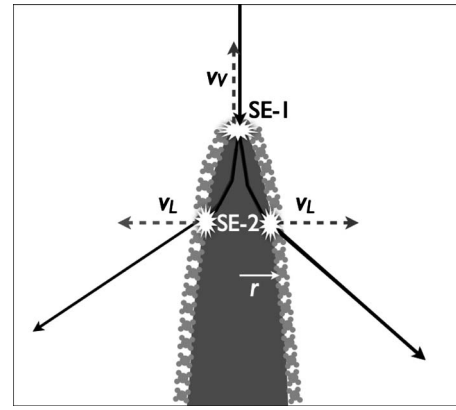


Fig. 5. Sketch of a simplified model for He-IBID pillar growth. The incident ions and their related secondary electrons of type 1 (SE-1) cause vertical pillar growth at a rate of v_v . The outgoing scattered ions and their related secondary electrons of type 2 (SE-2) cause lateral growth at a rate of v_L . Growth rates depend on the level of precursor depletion at the apex, which in turn depend on the ion current.

the deposition cross-section σ_i .¹ As stated above, we separate the growth into vertical growth, induced by SE-1 electrons (thus neglecting the incident ions), and lateral growth, induced by SE-2 electrons (thus neglecting the escaping scattered ions). Apart from the initial phase when SE-1 contribute to lateral growth as well, the lateral growth rate $v_L(t; i) (= dr/dt)$ of the pillar radius is thus

$$v_L(t; i) = \frac{dr}{dt} = \Delta V \Phi_2 n_s \sigma_2, \quad (4)$$

where n_s is the precursor density at the pillar's sidewall surface. We assume that this density is independent of current. Furthermore, we assume that the escaping ions originate from a line source, viz., the vertical symmetry axis of the pillar. The flux Φ_2 of SE-2s is given by the primary current, the number η_2 of emitted SE-2s per ion, the ion range R , and the circumference of the cone ($2\pi r$) as follows:

$$\frac{dr}{dt} \approx \Delta V \frac{\eta_2}{2\pi r R} \frac{i}{e} n_s \sigma_2 \equiv \frac{k_s i}{2r}, \quad (5)$$

where $k_s = \Delta V \eta_2 n_s \sigma_2 / e \pi R$. The solution of this differential equation is

$$r(t; i) = \sqrt{k_s i t + r_0^2}. \quad (6)$$

The integration constant r_0^2 reflects the pillars' initial lateral growth, mainly induced by the SE-1s. Combining Eqs. (3) and (6) yields for the final pillar radius r_f the following:

$$r_f(i) = \sqrt{\frac{k_s i R}{v_v} + r_0^2} = \sqrt{\frac{k_s (i + i_t) R}{v_\infty} + r_0^2}. \quad (7)$$

If there is depletion at the pillars' apex, the vertical and lateral growth induced by SE-1s are reduced by the same factor. Hence, r_0^2 is a constant, independent of the current i . The solid curve in Fig. 3 shows $2r_f(i)$ according to Eq. (7). The best fit to the data is obtained for $k_s = 360 \pm 25$ nm²/pC and $r_0 = 8 \pm 5$ nm. We conclude that the relative contribution to

the pillar volume by the initial SE-1 deposition, $(r_0/r_f(i))^2$, is small: ranging from 25% at 0.6 pA to 7% at 5 pA.

We derive from Eq. (7) the deposition efficiency, i.e., the volume V^* per incident ion ($V^* \sim \pi r^2 H e / Q$),

$$V^*(i) = \Delta V \eta_2 n_s \sigma_2 + \frac{\pi r_0^2 H(i) e}{Q} = \Delta V \eta_2 n_s \sigma_2 + \frac{\pi r_0^2 v_{\infty} e}{i + i_t}. \quad (8)$$

Note that we have used Eq. (2) here. The solid curve in Fig. 4 represents Eq. (8), where the first term, $\Delta V \eta_2 n_s \sigma_2$, was fitted to the data, thus producing the value $0.035 \pm 0.005 \text{ nm}^3/\text{ion}$. The model thus confirms the weak dependence of the deposition efficiency on the beam current, despite the concurrent strong variation in pillar shape.

Our model results can be compared to recent He-IBID Monte Carlo simulations of pillar growth for the same experimental data set.⁹ These simulations show good agreement with the experimental pillar shapes and confirm that, for the precursor-limited regime, the large majority of growth is indeed induced by SE-2s and scattered ions.

There are several uncertainties and approximations in our analytical approach. We discarded precursor depletion on the pillars' sidewalls, surface diffusion, inhomogeneities in the SE-2 flux, and the minor effects of sputtering. Nevertheless, Monte Carlo simulations show that the average depletion at the sidewalls is approximately 25%,⁹ whereas that at the apex is almost 90%. Assuming a Pt-to-C mass ratio of 4:1 (Ref. 6) and a mass density of 4.5 g/cm^3 ,⁹ the measured volumetric deposition yield of $0.04 \text{ nm}^3/\text{ion}$ corresponds to a deposition yield of 2.2 atoms/ion.

V. CONCLUSIONS

In general, IBID with focused He^+ beams produces sharper nanopillars than conventional focused Ga^+ beams can do. Pillars grown at high helium-ion currents are shorter and broader, but their volume is only slightly less than those grown at lower currents. The current dependence of the height is well described by a model for the transition from the ion-limited to the precursor-limited regime. Pillar broadening is a direct consequence of this transition. With increas-

ing beam current, depletion at the tip apex reduces the vertical growth rate, allowing more time for lateral growth. Assuming no precursor depletion at the pillar sidewalls, the broadening of the He-IBID pillars can be described by an analytical model for precursor decomposition. In this model, the primary ions and SE-1 electrons contribute to vertical growth, whereas the forward- and backward-scattered ions and the SE-2 electrons contribute to lateral growth. The final pillar width is proportional to the square root of the current plus an offset. Whether a similar approach can be applied to the study of pillars grown by Ga-IBID remains an open question. The growth mechanism for Ga-IBID is probably very different, i.e., induced by atomic collisions and not by secondary electrons. Furthermore, there is considerable sputtering during gallium-induced growth, and the compositions of helium and gallium-deposited materials differ significantly. Nevertheless, the simple analytical model may help to select optimal growth conditions and to understand detailed Monte Carlo simulations.

ACKNOWLEDGMENT

This research is part of NanoNed, a national research program on nanotechnology funded by the Ministry of Economic Affairs in The Netherlands.

¹I. Utke, P. Hoffmann, and J. Melngailis, *J. Vac. Sci. Technol. B* **26**, 1197 (2008).

²P. Chen, P. F. A. Alkemade, and H. W. M. Salemink, *Jpn. J. Appl. Phys.* **47**, 5123 (2008).

³J. Morgan, J. Notte, R. Hill, and B. Ward, *Microscopy Today*, **14**, 24 (2006).

⁴B. W. Ward, J. A. Notte, and N. P. Economou, *J. Vac. Sci. Technol. B* **24**, 2871 (2006).

⁵V. Sidorkin, E. van Veldhoven, E. van der Drift, P. F. A. Alkemade, H. W. M. Salemink, and D. Maas, *J. Vac. Sci. Technol. B* **27**, L18 (2009).

⁶C. A. Sanford, L. Stern, L. Barriss, L. Farkas, M. DiManna, R. Mello, D. J. Maas, and P. F. A. Alkemade, *J. Vac. Sci. Technol. B* **27**, 2660 (2009).

⁷D. A. Smith, J. D. Fowlkes, and P. D. Rack, *Nanotechnology* **18**, 265308 (2007).

⁸P. Chen, Ph.D. thesis, Delft University of Technology, 2010.

⁹P. Chen, E. van Veldhoven, C. A. Sanford, H. W. M. Salemink, D. Maas, D. A. Smith, P. D. Rack, and P. F. A. Alkemade, *Nanotechnology* **21**, 455302 (2010).

¹⁰V. Scheuer, H. Koops, and T. Tschudi, *Microelectron. Eng.* **5**, 423 (1986).